



## Facile measurement of polypeptide $J_{\text{HNH}\alpha}$ coupling constants from HMQC-J spectra

David S. Wishart\* & Yunjun Wang

Faculty of Pharmacy and Pharmaceutical Sciences, University of Alberta, Edmonton, AB, Canada T6G 2N8

Received 15 August 1997; Accepted 10 November 1997

*Key words:* coupling constant, heteronuclear, HMQC-J, linewidth, polypeptide

### Abstract

A method, based on linewidth measurements, is described which permits the rapid and facile determination of  $J_{\text{HNH}\alpha}$  coupling constants from  $^{15}\text{N}$  labeled proteins. Using appropriately processed HMQC-J data, we have found that a simple linear relationship exists between the half-height linewidth ( $\Delta\nu_{1/2}$ ) of  $^{15}\text{N}$ - $^1\text{H}$  cross peaks and their corresponding  $J_{\text{HNH}\alpha}$  coupling constants. Tests indicate that this technique permits the accurate measurement of up to 100  $J_{\text{HNH}\alpha}$  coupling constants in less than 30 min. Furthermore, the  $J_{\text{HNH}\alpha}$  measurements can be done manually – without the need of any computer-based curve-fitting or minimization. Comparisons between  $J_{\text{HNH}\alpha}$  values predicted from high resolution X-ray structures and those determined using this technique indicate that the method is both accurate and precise (correlation coefficient = 0.90, rmsd = 0.75 Hz).

*Abbreviations:*  $\Delta\nu_{1/2}$ , linewidth at half-height; DSS, 2,2-dimethyl-2-silapentane-5-sulfonic acid; HMQC, heteronuclear multiple quantum correlation spectroscopy; kDa, kilodaltons; MW, molecular weight; NOESY, nuclear Overhauser effect spectroscopy; rmsd, root-mean-square deviation; TOCSY, total correlation spectroscopy.

### Introduction

Since its introduction in 1989 (Kay et al., 1989; Kay and Bax, 1990) the HMQC-J experiment has emerged as one of the most popular methods for extracting precise  $J_{\text{HNH}\alpha}$  coupling constants from polypeptide spectra. By taking advantage of the longer  $T_2$  relaxation time found for  $^{15}\text{N}$  nuclei, Kay and co-workers were able to show that a highly digitized HMQC experiment could provide sufficient resolution to accurately measure  $J_{\text{HNH}\alpha}$  coupling constants. This remarkably simple approach, which exploits two key advantages of  $^{15}\text{N}$  nuclei (wide chemical shift dispersion and long  $T_2$ 's), has inspired the development of a host of other heteronuclear experiments for J-coupling measurement (Billeter et al., 1992; Vuister and Bax, 1993; Weisemann et al., 1994).

While the HMQC-J experiment is relatively trivial to implement, the extraction of coupling constants

from HMQC-J data is not quite so simple. The strong resolution enhancement required to differentiate in-phase doublets introduces two major problems: (i) reduced signal intensity and (ii) non-linearity in the relationship between  $J_{\text{HNH}\alpha}$  and the peak-to-peak separation. While little can be done to address the issue of reduced signal-to-noise, three different computational methods have been proposed to deal with the problem of non-linearity (Forman-Kay et al., 1990; Kay and Bax, 1990; Goodgame and Geer, 1993). Essentially all three approaches require the spectroscopist to process HMQC-J spectra using a progressive array of line-narrowing (resolution enhancement) filters. By measuring how the peak-to-peak separation changes as a function of the line-narrowing filters and then fitting these results to a simulated curve, it is possible to determine  $J_{\text{HNH}\alpha}$  values to relatively good accuracy. However, this iterative fitting process can be both tedious and error-prone. For instance, with the procedure of Goodgame and Geer, a 150-residue protein would require measuring and recording the peak-to-

\* To whom correspondence should be addressed.

peak separation of approximately 900 ( $6 \times 150$ ) doublets. In our hands, this protocol often requires a very full day (8–10 h) of intensive data processing and it often leads to inconsistent results.

In this paper we wish to describe a very simple technique which permits the accurate measurement of J-coupling constants from HMQC-J data in a fraction of the time required by other methods. Previously (Wang et al., 1997), we demonstrated how coupling constants could be rapidly extracted from half-height linewidth measurements of unresolved doublets from either TOCSY or NOESY spectra. We have since found that this linewidth measurement protocol can be applied to HMQC-J data (both in the F1 and F2 dimensions) with equal accuracy and precision. In particular, when compared to  $J_{\text{HNH}\alpha}$  data predicted from high resolution X-ray structures, the coupling constants measured with this simple linewidth technique have a correlation coefficient of 0.90 and an rmsd error of less than 0.75 Hz.

## Methods

### A. Experimental

HMQC-J data were obtained for a total of six proteins, all but one of which had a high resolution ( $< 2.0 \text{ \AA}$ ) X-ray crystal structure. The samples included  $^{15}\text{N}$ -labeled (1) *Escherichia coli* thioredoxin, (2) type III antifreeze protein from Ocean Pout, (3) type II antifreeze protein from Sea Raven, (4) *Bacillus circulans* xylanase, (5) turkey apo-troponin C (N domain) and (6) calcium-saturated troponin C (E41A-N domain) from turkey. Data were collected at temperatures ranging from 20–35 °C on two different Varian 500 spectrometers, each equipped with a 5 mm triple resonance probe.  $^1\text{H}$ - $^{15}\text{N}$  HMQC-J experiments (Kay and Bax, 1990) were typically performed with a  $^{15}\text{N}$  sweepwidth of 2000 Hz and a  $^1\text{H}$  sweepwidth of 6000 Hz. A total of 2048 complex points were collected along the  $t_2$  domain ( $^1\text{H}$ ) and 360–400 increments along the  $t_1$  domain ( $^{15}\text{N}$ ). The relaxation delays for these experiments were typically 1.2–2.5 s and the refocusing delay was set at between 4.9–5.3 ms. Data in both dimensions were zero-filled to create a  $4\text{K} \times 4\text{K}$  data set which was further processed using a shifted sine-bell weighting function (see details below). All  $^1\text{H}$ - $^{15}\text{N}$  HMQC-J spectra were referenced to internal DSS (Wishart et al., 1995).

Each HMQC-J spectrum was assigned on the basis of previously published chemical shift values (with

suitable corrections for pH and temperature). In particular,  $^1\text{H}/^{15}\text{N}$  assignments for *E. coli* thioredoxin were based on chemical shifts reported by Wishart (1991) and Chandrasekhar et al. (1991),  $^1\text{H}/^{15}\text{N}$  assignments for the apo and calcium-saturated forms of troponin C (N-domain) were from Gagne et al. (1994),  $^1\text{H}/^{15}\text{N}$  assignments for *B. circulans* xylanase were obtained from those reported by Plesniak et al. (1996),  $^1\text{H}/^{15}\text{N}$  assignments for type III antifreeze protein were from Sonnichsen et al. (1996, personal communication) and the  $^1\text{H}/^{15}\text{N}$  assignments for type II antifreeze protein were supplied by Dr. Wolfram Gronwald (personal communication).

In calculating the coupling constants for each polypeptide, we made use of the following Protein Data Bank entries (see Table 1): *E. coli* thioredoxin (2TRX), *B. circulans* xylanase (1BCX) and chicken troponin C (1NCZ). The crystal structure coordinates for type III antifreeze protein were generously provided by Dr. Zongchao Jia of Queens University (personal communication). The coordinate set for chicken troponin C (1NCZ) was chosen over that of turkey troponin C (5TNC) for two reasons: (1) it was of higher quality (better resolution, lower R factor) and (2) the amino acid sequences for the two species are identical, implying that the 3D structures should also be identical. We also assumed (based on the recent work of Gagne et al., 1997) that the apo- and calcium-loaded forms would have essentially identical structures (save for a small rotation of one bond and a single residue substitution of another) and that one crystal structure would suffice for both the apo and calcium-loaded forms.

$J_{\text{HNH}\alpha}$  coupling constants for each of the above crystal structures were predicted from the reported backbone  $\phi$  angles using the following equation:  $J = 5.9 \cos^2 \theta - 1.3 \cos \theta + 2.2$ , where  $\theta = |\phi - 60^\circ|$  (see Wang et al., 1997 for more details on the derivation of this equation). Use of other widely used Karplus parameters (Pardi et al., 1984; Vuister and Bax, 1993; Wang and Bax, 1996) led to only minor differences in the overall performance of this method. Note that because a crystal structure is not yet available for the type II antifreeze protein, we used the  $J_{\text{HNH}\alpha}$  coupling constants measured from a separate HNHA experiment (Vuister and Bax, 1993) as a proxy for the X-ray crystal values.

Table 1. Listing of high resolution X-ray structures used in calculating  $J_{X\text{-ray}}$  values

Protein	Accession	Resolution (Å)	R-factor	Reference
Thioredoxin ( <i>E. coli</i> )	2TRX	1.68	0.165	Katti et al. (1990)
Troponin C (Apo)	1NCZ	1.80	0.19	Satyshur et al. (1994)
Troponin C (E41A)	1NCZ	1.80	0.19	Satyshur et al. (1994)
Xylanase ( <i>B. circulans</i> )	1BCX	1.80	0.163	Wakarchuk et al. (1994)
Antifreeze protein (III)	N/A	1.25	0.14	Z. Jia (personal communication)

### B. Determination of $J_{\text{HNH}\alpha}$ coupling constants from $\Delta\nu_{1/2}$

The protocol for determining  $J_{\text{HNH}\alpha}$  coupling constants for HMQC-J data is very similar to the procedure described earlier for analyzing TOCSY or NOESY spectra (Wang et al., 1997). As stated previously, the spectral resolution prior to zero-filling in both the F2 and F1 dimensions should be better than 6.0 Hz/pt. After base-line correction and zero-filling to produce a 4K × 4K data set, a sine-bell weighting function of the form:

$$\sin^2[\pi(t - \text{sbs})/2\text{sb}] \quad (1)$$

should be applied (where sb and sbs are given in seconds). For Varian spectrometers running VNMR software (Version 5.1 or higher)  $\text{sb} = \text{sb1} = -0.100$  and  $\text{sbs} = \text{sbs1} = -0.066$ . Note that the negative signs preceding sb and sb1 are used by Varian software to denote a sine-bell ‘squared’ function. For other kinds of spectral processing software, please refer to the conversion formulae provided by Wang et al. (1997).

After processing and assigning the spectrum, one can select traces either from the F1 ( $^{15}\text{N}$ ) or F2 ( $^1\text{H}$ ) dimension and subsequently determine the half-height linewidth ( $\Delta\nu_{1/2}$ ) for each assigned  $^1\text{H}$ - $^{15}\text{N}$  cross peak. For Varian spectrometers the command ‘dres’ automatically determines  $\Delta\nu_{1/2}$  for any given trace. For Bruker spectrometers,  $\Delta\nu_{1/2}$  determination takes slightly more effort. By substituting the measured half-width at half-height ( $\Delta\nu_{1/2}$ ) for F1 ( $^{15}\text{N}$ ) traces into the following equation:

$$J_{\text{HNH}\alpha} = 0.45(\Delta\nu_{1/2}) - \text{MW}/20\,000 \quad (2)$$

or the measured half-width at half-height ( $\Delta\nu_{1/2}$ ) for F2 ( $^1\text{H}$ ) traces into this equation:

$$J_{\text{HNH}\alpha} = 0.50(\Delta\nu_{1/2}) - \text{MW}/10\,000 \quad (3)$$

the  $J_{\text{HNH}\alpha}$  coupling constant can be determined. Note that  $\Delta\nu_{1/2}$  is the half-height linewidth (measured in

Hz) of a given  $^1\text{H}$ - $^{15}\text{N}$  resonance and MW is the apparent molecular weight of the protein in daltons. Equations (2) and (3) work well in most situations. However, care must be taken in using the correct molecular weight (i.e. is the polypeptide of interest a monomer or a dimer at NMR concentrations?) and making sure that the temperature of the sample is between 20 °C and 35 °C. Under certain circumstances, the situation can be complicated by the presence of inherently broad linewidths, poor shimming, paramagnetic contaminants or the use of unusually high (>40 °C) or low (< 15 °C) temperatures.

A second approach, which eliminates the problems associated with intrinsic linewidth, temperature or sample differences, can also be used to determine  $J_{\text{HNH}\alpha}$ . This method is based on the observation that the narrowest  $^1\text{H}$ - $^{15}\text{N}$  resonance invariably has a  $J_{\text{HNH}\alpha}$  coupling constant of close to 4.0 Hz. This phenomenon was observed for all six protein samples used in this study and for all 11 polypeptides used in our earlier report (Wang et al., 1997). Using this observation, we have found that  $J_{\text{HNH}\alpha}$  can be determined using either one of the two following equations:

$$J_{\text{HNH}\alpha} = 0.45(\Delta\nu_{1/2}) - 0.45(\Delta\nu_{1/2}(\text{min})) + 4.0 \quad (4)$$

for  $^{15}\text{N}$  traces,

$$J_{\text{HNH}\alpha} = 0.50(\Delta\nu_{1/2}) - 0.50(\Delta\nu_{1/2}(\text{min})) + 4.0 \quad (5)$$

for  $^1\text{H}$  traces, where  $\Delta\nu_{1/2}$  is the half-height linewidth (in Hz) of a given  $^1\text{H}$ - $^{15}\text{N}$  resonance and  $\Delta\nu_{1/2}(\text{min})$  is the half-height linewidth (in Hz) of the narrowest  $^1\text{H}$ - $^{15}\text{N}$  resonance in the spectrum. A small disadvantage to this approach is that coupling constants cannot be determined until after all of the resonance linewidths have been measured and the narrowest line identified. Furthermore, this protocol cannot be applied to the measurement of unstructured peptides or

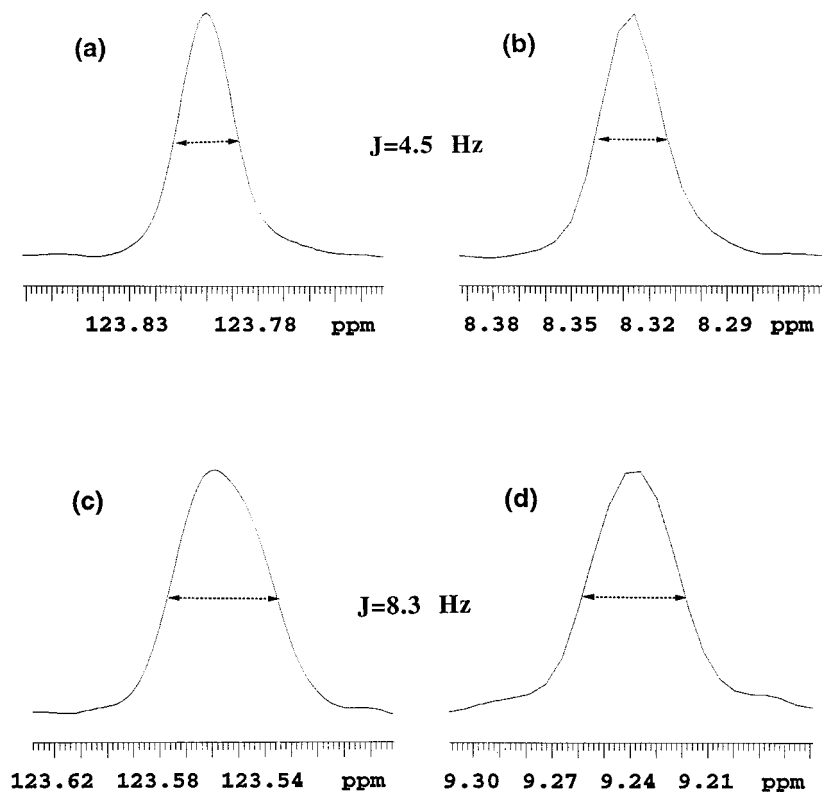


Figure 1. Four examples of traces taken through  $^1\text{H}$ - $^{15}\text{N}$  cross peaks from an HMQC-J spectra of *B. circulans* xylanase. Illustrated in (a) and (b) are the traces of Lys<sup>154</sup> taken through the  $^1\text{H}$  (F2) dimension and  $^{15}\text{N}$  (F1) dimension respectively. The measured half-height linewidth in (a) was 12.1 Hz, while the measured half-height linewidth in (b) was 13.4 Hz. Illustrated in (c) and (d) are the traces of Val<sup>98</sup> taken through the  $^1\text{H}$  (F2) dimension and  $^{15}\text{N}$  (F1) dimension respectively. The measured half-height linewidth in (c) was 19.7 Hz, while the measured half-height linewidth in (d) was 18.8 Hz. The  $J_{\text{HNH}\alpha}$  value (in Hz) as predicted from high resolution X-ray data is indicated in each figure. Note that broad peaks are associated with large coupling constants while narrow peaks are associated with small coupling constants.

denatured proteins. In these situations the narrowest amide cross peak would likely correspond to a coupling constant of 6 or 7 Hz instead of 4.0 Hz.

## Results

Figure 1 illustrates four examples of traces taken through various  $^1\text{H}$ - $^{15}\text{N}$  cross peaks. As can be seen in these four examples, the  $\Delta\nu_{1/2}$  is closely related to the measured  $J_{\text{HNH}\alpha}$  coupling value, with large  $\Delta\nu_{1/2}$  values corresponding to large coupling constants and small  $\Delta\nu_{1/2}$  values corresponding to small coupling constants. This relationship holds regardless of whether one is measuring in the F1 ( $^{15}\text{N}$ ) or the F2 ( $^1\text{H}$ ) dimension. It can be further verified if we plot the relationship between  $\Delta\nu_{1/2}$  and the  $J_{\text{HNH}\alpha}$  coupling constant as derived from X-ray data. In Figure 2 we illustrate the linear relationship that exists between

$\Delta\nu_{1/2}$  (measured along either the  $^1\text{H}$  axis or the  $^{15}\text{N}$  axis) and  $J_{\text{HNH}\alpha}$  for all measurable resonances from an HMQC-J spectrum of the N domain of turkey apotroponin C. An excellent fit is obtained for both sets of measurements with correlation coefficients ( $r$ ) of 0.94 for F2 ( $^1\text{H}$ ) traces and 0.93 for F1 ( $^{15}\text{N}$ ) traces. The strong correlation between  $\Delta\nu_{1/2}$  and  $J_{\text{HNH}\alpha}$  and the linear relationship observed for these and other examples suggested that a simple equation of the form:

$$J_{\text{HNH}\alpha} = m * \Delta\nu_{1/2} + B \quad (6)$$

(where  $m$  is the slope,  $B$  is the y intercept and  $\Delta\nu_{1/2}$  is the half-height linewidth) could be developed to predict coupling constants from  $\Delta\nu_{1/2}$  measurements of HMQC-J spectra. Simulations, using the weighting functions described here and  $^1\text{H}/^{15}\text{N}$   $T_2$ 's typical of many mid-sized proteins, confirm that this linear approximation is valid (Figure 3).

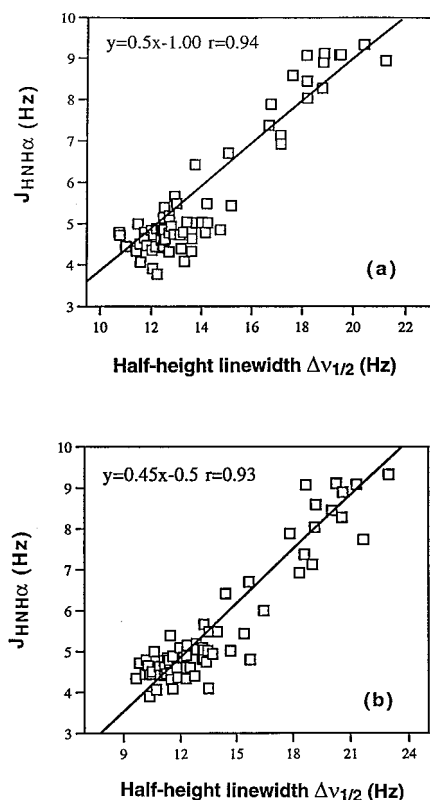


Figure 2. Relationship between  $\Delta v_{1/2}$  and the predicted  $J_{\text{HNH}\alpha}$  (from X-ray data) for apo-troponin C as determined from (a)  $^1\text{H}$  (F2) traces and (b)  $^{15}\text{N}$  (F1) traces respectively. The equations for the 'best-fit' line derived from the molecular weight based approach and the correlation coefficients ( $r$ ) are shown in the top left corner of each graph. Note that the superimposed curve is a 'best fit' line for all of the data (390 points) and all of the proteins (six) and so, for any given protein, there may be slight systematic deviations at certain extrema.

Obviously, for this method to work effectively it is important to be able to determine the  $y$ -intercept (B) independently of the measured linewidths. In Figure 4 we illustrate how these intercepts can be so determined. In Figure 4(a) the relationship between the 'best-fit'  $y$ -intercept and the molecular weight of each protein is plotted. Note that the calcium-saturated E41A mutant of troponin C (N-domain) forms a dimer in the presence of calcium ( $\text{MW}_{\text{dimer}} = 19.8$  kDa), and that type II antifreeze protein ( $\text{MW}_{\text{dimer}} = 28.1$  kDa) also showed strong evidence of dimer formation under the conditions used in this study. The remaining compounds are known to be monomeric. Also plotted in Figure 4(b) is the relationship between the 'best-fit'  $y$ -intercept and the half-height linewidth of the narrowest line ( $\Delta v_{1/2}(\text{min})$ ). With the exception of *B. circulans* xylanase, which exhibited an unusual

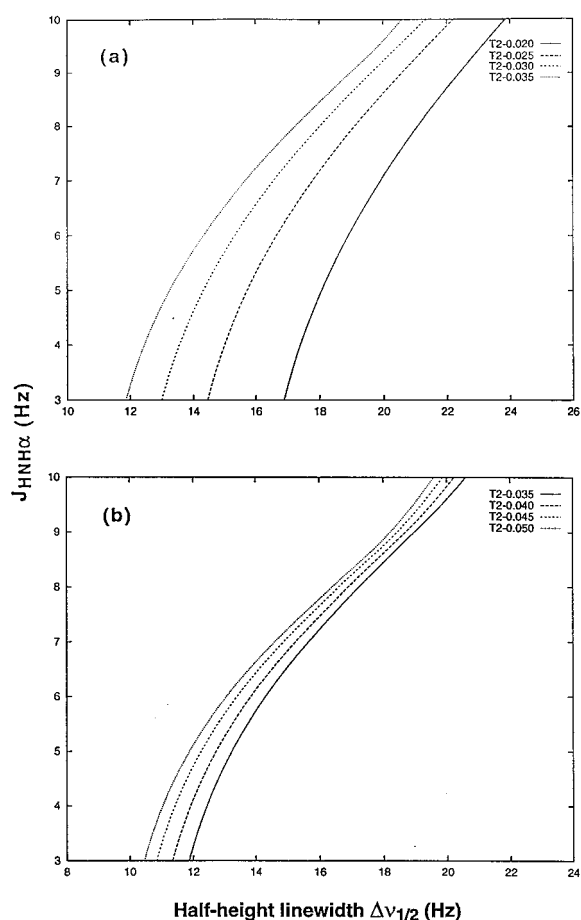


Figure 3. Computer simulation of the relationship between  $\Delta v_{1/2}$  and  $J_{\text{HNH}\alpha}$  coupling constants for (a)  $^1\text{H}$  traces and (b)  $^{15}\text{N}$  traces using  $T_2$  values typical of mid-sized proteins and the sine-bell processing parameters suggested in the text. Note that while both sets of simulated curves are slightly parabolic, a linear approximation appears to fit the experimental data quite well (see Figure 2).

linewidth distribution, the straight-line fits to these plots are excellent.

Despite the small problem with xylanase, use of the equations presented here would still allow one to accurately predict the coupling constants of this protein as seen by the data presented in Tables 2 and 3. These two tables summarize the correlation between these predicted coupling constants (designated as  $J_{\text{lw}}$  – since they were derived from linewidth measurements) and the coupling constants predicted from the corresponding high resolution X-ray structures (designated as  $J_{\text{x-ray}}$ ). In assembling these two tables a total of more than 750 coupling constant measurements (387 from  $^1\text{H}$  traces; 378 from  $^{15}\text{N}$  traces) were made. Both tables clearly show the excellent agreement obtained

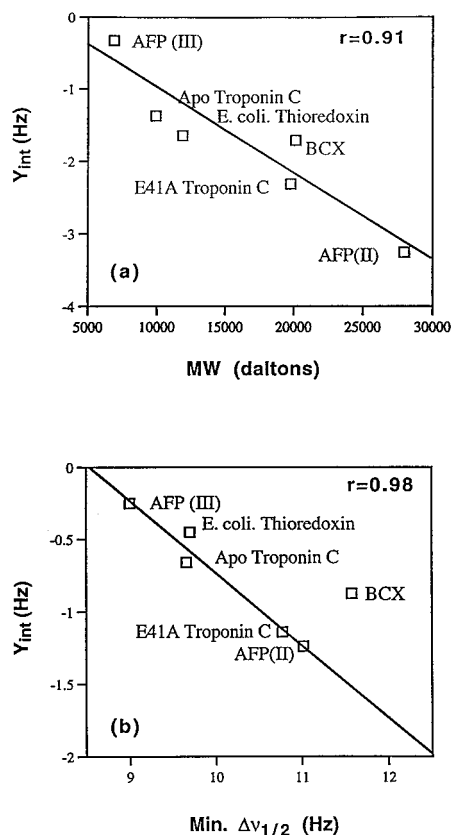


Figure 4. (a) Relationship between the 'best-fit' y-intercept and the molecular weight of each of the test proteins derived from  $^1\text{H}$  linewidth measurements and (b) the relationship between the 'best-fit' y-intercept and the linewidth of the narrowest amide resonance for each test protein derived from  $^{15}\text{N}$  linewidth measurements. The correlation coefficient (excluding BCX in the lower figure) is given in the top right corner of each graph.

for both large (28 kDa) and small (7 kDa) proteins using traces from either the  $^1\text{H}$  or  $^{15}\text{N}$  dimension. Overall, for the six proteins tested,  $^1\text{H}$  linewidth measurements yielded an average correlation coefficient of 0.89 and an rmsd from  $J_{X\text{-ray}}$  of 0.77 Hz while  $^{15}\text{N}$  linewidth measurements yielded an average correlation coefficient of 0.90 and an rmsd from  $J_{X\text{-ray}}$  of 0.73 Hz.

## Discussion

In assessing the accuracy of the method presented here, it is important to remember the limitations inherent in comparing X-ray structures with NMR solution structures. Wang and Bax (1996) and Wang et al. (1997) discuss, in some detail, what should be expected in terms of correlation coefficients ( $r$ ) and rms

deviations between X-ray-derived and experimentally measured coupling constants. Suffice it to say that given the limitations of resolution, thermal motion and signal-to-noise for both techniques, a 'perfect' method could probably expect to do no better than  $r = 0.97$  and an rmsd = 0.54 Hz between  $J_{X\text{-ray}}$  and  $J_{\text{NMR}}$ . Wang et al. (1997) suggest that a more realistic expectation of ideality would be  $r = 0.93$  and an rmsd = 1.04 Hz between  $J_{X\text{-ray}}$  and  $J_{\text{NMR}}$ .

As can be seen from Tables 2 and 3, our experimentally measured  $J_{\text{W}}$  values compare very favorably with the results from our earlier method (Wang et al., 1997) developed explicitly for TOCSY and/or NOESY spectra ( $r = 0.89$  and rmsd = 0.85 Hz). They also compare favorably with the original HMQC-J results (based on peak-to-peak measurements) reported by Kay et al. (1989) for staphylococcal nuclease ( $r = 0.89$  and rmsd = 1.01 Hz). The HNHA method of Vuister and Bax (1993) as applied to staphylococcal nuclease yielded an  $r$  value of 0.91 and an rmsd = 0.76 Hz. Later measurements with an expanded data set (Garrett et al., 1994) found that the HNHA experiment produced an agreement between X-ray and NMR results having an  $r$  value of 0.78 and an rmsd of 1.42 Hz. The J-modulated COSY approach developed by Billeter et al. (1992) as applied to the 434 repressor protein produced an  $r = 0.92$  and an rmsd = 0.76 Hz.

Overall, there is little to distinguish between these methods. Nearly all of the approaches (including the one described here) achieve a level of agreement that is reasonably close to 'ideal' (rmsd = 1.04 Hz,  $r = 0.93$ ). While some methods perform slightly better than ours (0.92 vs. 0.90), it is important to note that our calculations were performed on a substantially larger sample (5 to 15 times larger) and a significantly more diverse set of polypeptides (in both size and structure) than any of the other methods. We expect that if the other approaches were applied to a comparably large or diverse data set, their performance would be similarly compromised (see Garrett et al., 1994).

While the above analysis largely confirms that the accuracy and precision of this new approach are as good as any other method currently in use, we believe that the simplicity and rapidity with which J-coupling constants can be determined should make this method particularly appealing to spectroscopists. Specifically, this technique offers four key advantages: (i) the collection and processing of the HMQC-J spectrum only needs to be performed once (as opposed to six or seven times), (ii) the conversion of linewidth measurements to coupling constants can often be done in

Table 2. Summary of results obtained using linewidth analysis for determination of  $J_{\text{HNH}\alpha}$  coupling constants ( $^1\text{H}$  dimension only)

Protein	MW (Da)	No. of points	$r$ ( $J_{\text{X-ray}}$ vs $J_{\text{JW}}$ )	rmsd ( $J_{\text{X-ray}}$ vs $J_{\text{JW}}$ )
Antifreeze protein (III)	6860	50	0.92	0.71
Troponin C (Apo)	9900	69	0.94	0.59
Thioredoxin ( <i>E. coli</i> )	11880	56	0.91	0.82
Troponin C (E41A)	19800	60	0.88	0.73
Xylanase ( <i>B. circulans</i> )	20400	108	0.84	0.83
Antifreeze protein (II)	28000	44	0.91	0.95

Table 3. Summary of results obtained using linewidth analysis for determination of  $J_{\text{HNH}\alpha}$  coupling constants ( $^{15}\text{N}$  dimension only)

Protein	MW (Da)	No. of points	$r$ ( $J_{\text{X-ray}}$ vs $J_{\text{JW}}$ )	rmsd ( $J_{\text{X-ray}}$ vs $J_{\text{JW}}$ )
Antifreeze protein (III)	6860	52	0.93	0.67
Troponin C (Apo)	9900	67	0.93	0.58
Thioredoxin ( <i>E. coli</i> )	11880	50	0.93	0.74
Troponin C (E41A)	19800	57	0.83	0.82
Xylanase ( <i>B. circulans</i> )	20400	108	0.88	0.71
Antifreeze protein (II)	28000	44	0.91	0.92

one's head, (iii) the measurement of linewidths can be accomplished quickly and easily (typically 100 measurements in 30 min); and (iv) the  $J_{\text{HNH}\alpha}$  coupling constants can be extracted from both the  $^1\text{H}$  and the  $^{15}\text{N}$  dimension. This latter point illustrates the robustness of this new approach because it allows one to confirm a coupling constant measurement in two independent ways – one from a  $^{15}\text{N}$  trace and the other from a  $^1\text{H}$  trace – using only a single cross peak. Direct comparisons between the  $J_{\text{HNH}\alpha}$  values derived from the two traces (F1 and F2) show that they are highly correlated ( $r = 0.95$ ) and this further suggests that if a trace in one dimension is obscured or distorted, then a trace in the other dimension (if it is not distorted or obscured) could be used to extract a coupling constant with a high degree of confidence.

While there are many positive aspects to this simple approach to  $J_{\text{HNH}\alpha}$  coupling constant determination, there are at least a few limitations that merit further discussion. One obvious shortcoming is the fact that, in order for this method to work, the HMQC-J spectra must be collected and processed in a very specific manner. While this can be a hindrance, the reprocessing of a previously collected HMQC-J spectrum (with modern computers) should only take a few seconds. On the other hand, competing methods based

primarily on computer-aided curve fitting ( Kay et al., 1989; Billeter et al., 1992; Goodgame and Geer, 1993; Vuister and Bax, 1993) are much more flexible and do not typically constrain the user to follow special collection and processing conditions. Another limitation of this linewidth-based technique arises from the fact that it can be sensitive to conditions that affect linewidths, but which may not necessarily affect  $J_{\text{HNH}\alpha}$  coupling constants. Such variables as temperature, paramagnetic contaminants, solvent viscosity, non-uniform segmental motion, dimerization events, intermediate exchange events, spectral overlap and decoupler distortion can all affect linewidth measurements – yet these phenomena often have little to do with a protein's average backbone structure or its  $J_{\text{HNH}\alpha}$  coupling constants. Consequently, these common sources of lineshape perturbation or distortion can potentially lead to incorrect  $J_{\text{HNH}\alpha}$  values. A third limitation lies with the potential difficulties associated with determining the 'y-intercept'. As seen with the *B. circulans* xylanase example, it is sometimes possible to introduce a systematic error (up to 0.5 Hz) in coupling constant measurements through an incorrect determination of the 'y-intercept' or correction factor. Care, therefore, must be taken to ensure that this correction factor is consistent with what is known about

the molecule and that it yields a range of  $J_{\text{HNH}\alpha}$  values typical for proteins (between 3 Hz and 10 Hz). Despite these possible limitations, we have found that this technique has worked very well for every protein so far tested.

## Conclusions

To summarize, we have described a novel method that allows  $J_{\text{HNH}\alpha}$  coupling constants to be rapidly determined from simple linewidth measurements in either the  $^1\text{H}$  or  $^{15}\text{N}$  dimension of HMQC-J cross peaks. This new method makes use of the linear relationship between  $J_{\text{HNH}\alpha}$  and half-height linewidths ( $\Delta\nu_{1/2}$ ) of appropriately processed NMR spectra. We believe this approach offers several advantages over other previously described heteronuclear techniques for extracting  $J_{\text{HNH}\alpha}$  coupling constants. In particular, it is simple, quick, accurate (having an rmsd of less than 0.8 Hz), easy to learn, applicable to both small and large proteins, independent of any requirement for specialized hardware, and independent of the spectrometer make, size or type. We believe that if this simple concept of linewidth measurement is widely adopted, it could make quantitative coupling constant measurements far simpler and far easier to use in analyzing the solution conformation of peptides, proteins, polynucleotides and other biomolecules via NMR.

## Acknowledgements

The authors wish to thank Lawrence P. McIntosh, Brian D. Sykes, Stephane M. Gagne, Frank D. Sonnichsen, Peter Davies and Zongchao Jia for their advice and assistance. We also wish to acknowledge Deborah J. Waldman for her help in preparing and proof-reading the manuscript. Financial support by the Natural Sciences and Engineering Research Council (Canada), the Protein Engineering Network of Centres of Excellence (Canada), Bristol Myers-Squibb (Canada) and the Alberta Heritage Foundation for Medical Research is gratefully acknowledged.

## References

- Bax, A., Vuister, G.W., Grzesiek, S., Delaglio, F., Wang, A.C., Tschudin, R. and Zhu, G. (1994) *Methods Enzymol.*, **239**, 79–105.
- Billeter, M., Neri, D., Otting, G., Qian, Y.Q. and Wüthrich, K. (1992) *J. Biomol. NMR*, **2**, 257–274.
- Chandrasekhar, K., Krause, G., Holmgren, A. and Dyson, H.J. (1991) *FEBS Lett.*, **284**, 178–183.
- Forman-Kay, J.D., Gronenborn, A.M., Kay, L.E., Wingfield, P.T. and Clore, M.G. (1990) *Biochemistry*, **29**, 1566–1572.
- Gagne, S.M., Li, M.X. and Sykes, B.D. (1997) *Biochemistry*, **36**, 4386–4392.
- Gagne, S.M., Tsuda, S., Li, M.X., Chandra, M., Smillie, L.B. and Sykes, B.D. (1994) *Protein Sci.*, **3**, 1961–1974.
- Garrett, D.S., Kuszewski, J., Hancock, T.J., Lodi, P.T., Vuister, G.W., Gronenborn, A.M. and Clore, G.M. (1994) *J. Magn. Reson.*, **B104**, 99–103.
- Goodgame, M.M. and Geer, S.M. (1993) *J. Magn. Reson.*, **A102**, 246–248.
- Katti, S.K., LeMaster, D.M. and Eklund, H. (1990) *J. Mol. Biol.*, **212**, 167–184.
- Kay, L.E. and Bax, A. (1990) *J. Magn. Reson.*, **86**, 110–126.
- Kay, L.E., Brooks, B., Sparks, S.W., Torchia, D.A. and Bax, A. (1989) *J. Am. Chem. Soc.*, **111**, 5488–5490.
- Pardi, A., Billeter, M. and Wüthrich, K. (1984) *J. Mol. Biol.*, **180**, 741–751.
- Plesniak, L.A., Wakarchuk, W.W. and McIntosh, L.P. (1996) *Protein Sci.*, **5**, 1118–1135.
- Satyshur, K.A., Pyzalska, D., Rao, S.T., Greaser, M. and Sundaralingam, M. (1994) *Acta Crystallogr. D*, **50**, 40–49.
- Sonnichsen, F.D., DeLuca, C.I., Davies, P.L. and Sykes, B.D. (1996) *Structure*, **4**, 1325–1337.
- Sonnichsen, F.D., Sykes, B.D., Chao, H. and Davies, P.L. (1993) *Science*, **259**, 1154–1157.
- Vuister, G.W. and Bax, A. (1993) *J. Am. Chem. Soc.*, **113**, 7772–7777.
- Wakarchuk, W.W., Cambell, R.L., Sung, W.L., Davoodi, J. and Yaguchi, M. (1994) *Protein Sci.*, **3**, 467–474.
- Wang, A.C. and Bax, A. (1996) *J. Am. Chem. Soc.*, **118**, 2483–2494.
- Wang, Y., Nip, A.M. and Wishart, D.S. (1997) *J. Biomol. NMR*, **10**, 373–382.
- Weisemann, R., Rüterjans, J., Schalbe, H., Schleucher, J., Bermel, W. and Griesinger, C. (1994) *J. Biomol. NMR*, **4**, 231–240.
- Wishart, D.S. (1991) Ph.D. Thesis, Yale University, New Haven, CT.
- Wishart, D.S., Bigam, C.G., Yao, J., Abildgaard, F., Dyson, H.J., Oldfield, E., Markley, J.L. and Sykes, B.D. (1995) *J. Biomol. NMR*, **6**, 135–140.